Quantification of Collagen Organization in the Peripheral Human Cornea at Micron-Scale Resolution

Craig Boote,[†] Christina S. Kamma-Lorger,[†] Sally Hayes,[†] Jonathan Harris,[†] Manfred Burghammer,[‡] Jennifer Hiller,[§] Nicholas J. Terrill,[§] and Keith M. Meek[†*]

[†]Structural Biophysics Group, School of Optometry and Vision Sciences, Cardiff University, Cardiff, United Kingdom; [‡]European Synchrotron Radiation Facility, Grenoble, France; and [§]Diamond Light Source, Didcot, United Kingdom

ABSTRACT   The collagen microstructure of the peripheral cornea is important in stabilizing corneal curvature and refractive status. However, the manner in which the predominantly orthogonal collagen fibrils of the central cornea integrate with the circumferential limbal collagen is unknown. We used microfocus wide-angle x-ray scattering to quantify the relative proportion and orientation of collagen fibrils over the human corneolimbal interface at intervals of 50 μm. Orthogonal fibrils changed direction 1–1.5 mm before the limbus to integrate with the circumferential limbal fibrils. Outside the central 6 mm, additional preferentially aligned collagen was found to reinforce the cornea and limbus. The manner of integration and degree of reinforcement varied significantly depending on the direction along which the limbus was approached. We also employed small-angle x-ray scattering to measure the average collagen fibril diameter from central cornea to limbus at 0.5 mm intervals. Fibril diameter was constant across the central 6 mm. More peripherally, fibril diameter increased, indicative of a merging of corneal and scleral collagen. The point of increase varied with direction, consistent with a scheme in which the oblique corneal periphery is reinforced by chords of scleral collagen. The results have implications for the cornea's biomechanical response to ocular surgeries involving peripheral incision.

INTRODUCTION

The cornea is unique among connective tissues in combining high mechanical strength with >90% transparency to visible light. This is made possible by the highly specialized organization of the corneal stroma, consisting primarily of collagen fibrils embedded in a hydrated extrafibrillar matrix (1). Transparency is achieved through the small, uniform diameter of fibrils and their high level of lateral order; whereas mechanical strength is provided by their gross arrangement within multiple lamellae that lie approximately parallel to the tissue surface (2). As the primary refractive component (3), the human cornea demands precise curvature, being almost spherical near the visual axis but flattening toward the limbus, the transition region between the cornea and less curved sclera. Although the basis of this contour is not well understood, corneal shape is likely influenced by differences in the specific size and arrangement of collagen fibrils between tissue regions (4). Determining how stromal collagen organization defines corneal shape is a key to understanding the biomechanical basis of refractive changes in response to disease and surgery.

X-ray scattering can quantitatively determine the bulk-thickness orientation (5) and diameter (6) of corneal fibrils, and has indicated a preferential orientation of collagen in the central human cornea, in which fibrils are distributed around the inferior-superior (i-s) and nasal-temporal (n-t) orthogonal meridians (7,8). In contrast, at the limbus the dominant fibril orientation is reported to be tangential, indicative of a pseudoannulus of collagen circumscribing the cornea (9). Recently, studies using serial limbal sections revealed that the bulk of the tangential x-ray scatter is restricted to the posterior stroma (10). At least a portion of this scatter is likely to be associated with Schwalbe's ring, a collagen annulus in the posterior stroma between the termination of Descemet's membrane and the trabecular meshwork (11). In addition, increased collagen scatter in the oblique corneal periphery (Fig. 1) has been attributed to the possible presence of additional anchoring lamellae of envisaged scleral origin (12,13). The idea of the scleral and corneal collagen intermingling is supported by fibril diameter (14,15) and transparency (16) measurements. However, notably, the existence of the theoretical anchoring fibrils has not been confirmed.

A number of theoretical (17–19) and experimental (18,20) studies have indicated that the collagen microstructure of the peripheral cornea plays an important role in stabilizing corneal curvature, yet the important question of how the predominantly i-s/n-t fibrils of the central stroma integrate with the apparently circumferential limbal collagen has not been adequately addressed. X-ray data are consistent with a scheme in which fibrils change direction near the corneal periphery (21,22), to run circumferentially (Fig. 2 A). However, the amount of collagen x-ray scatter increases with distance from the corneal center (22), raising the possibility that the pseudoannulus could be formed either by a separate population of straight (within the curved plane of the cornea; Fig. 2 B) or curved (Fig. 2 C) lamellae entering the cornea from the sclera at different angles, or
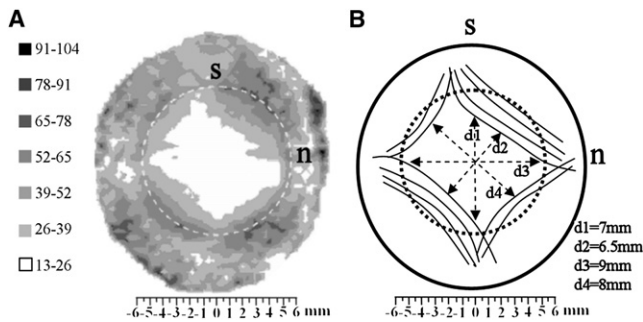
FIGURE 1   (*A*) Contour map of aligned collagen x-ray scatter (a.u.) from a right human cornea. Superior, s, and nasal, n, positions are marked. Broken line denotes the limbus. Note the skewed diamond shape of the scatter contours, which displays mirror symmetry between the left and right eyes. (*B*) Proposed model of collagen fibril arrangement to explain the shape of the aligned scatter contours. The peripheral, oblique cornea is reinforced by chords of anchoring collagen of scleral origin. Figure modified from Boote et al. (13).

alternatively by a discrete population of circular fibrils (Fig. 2 *D*). Furthermore, Pinsky et al. (23) propounded an alternative geometrical interpretation of the x-ray data based on geodesics (Fig. 2 *E*), while circular light polarization biomicroscopy (24) has inspired a further model in which corneal fibrils follow confocal elliptic/hyperbolic paths (Fig. 2 *F*). To address the uncertainty surrounding the integration of the corneal and limbal collagen, we carried out a detailed study using a combination of conventional and microfocus x-ray beam technology.

MATERIALS AND METHODS

Tissue

Two left human corneas (1 and 2) with scleral rim were obtained from the National Disease Research Interchange (Philadelphia, PA), and two right specimens (3 and 4) from the Bristol Eye Bank, UK. The donor ages were 71 years (Corneas 1 and 3), 98 years (Cornea 2), and 47 years (Cornea 4) and none had any previous history of corneal surgery or disease. All specimens were wrapped in polyvinylidene chloride film (Clingfilm, Superdrug Stores Plc., Croydon, UK) and stored frozen at −80°C. Immediately before x-ray experiments the specimens were thawed and the film wrap retained for the duration of the experiments to prevent tissue dehydration.

Microfocus wide-angle x-ray scattering

Wide-angle x-ray scattering (WAXS) data were collected from Corneas 1 and 2 on beamline ID13 at the European Synchrotron Radiation Facility (ESRF, Grenoble, France), using a microfocus x-ray beam (λ = 0.098 nm) measuring 0.02 mm (Cornea 1) or 0.01 mm (Cornea 2) in diameter. The film-wrapped specimens were placed separately inside sealed sample holders bounded by two sheets of Mylar film (DuPont Teijin Films, London, UK), with the anterior corneal surface facing the incident x-ray beam and the superior corneal position uppermost. The holder clamped the Clingfilm around the tissue, such that the Mylar windows were not in contact with the wrapped specimen, allowing the cornea to retain its natural curvature. An in-line microscope, calibrated with the x-ray beam position, was used for initial sample alignment before x-ray exposure. For Cornea 1,
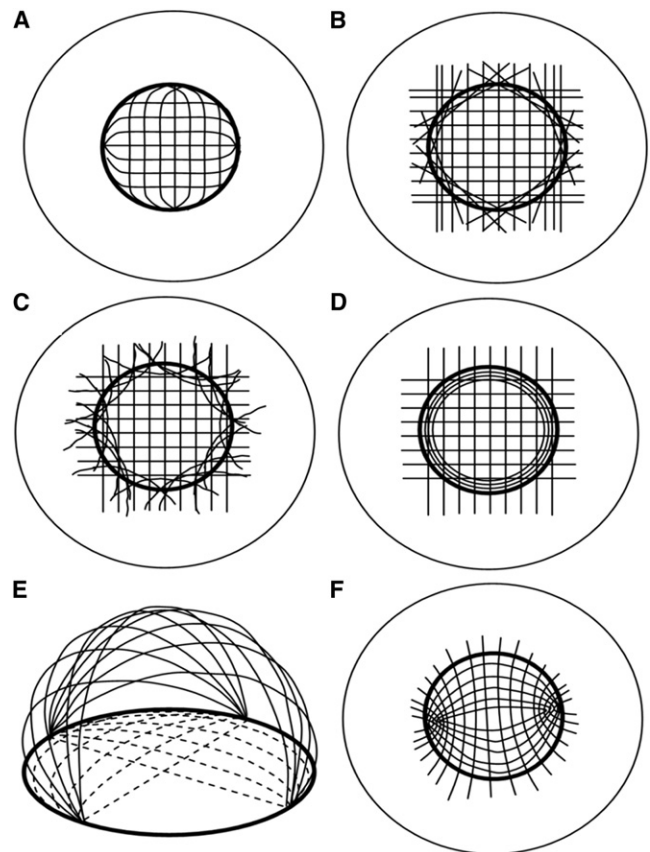

FIGURE 2   Previous models to explain the integration of corneal and limbal fibrils, based on data from (*A–E*) x-ray scattering and (*F*) circular polarization biomicroscopy. (*A*) The orthogonal fibrils change direction to form the limbal annulus. (*B*) A discrete population of straight, tangential scleral fibrils forms the pseudoannulus. (*C*) Discrete, curved scleral fibrils form the limbal annulus. (*D*) The limbal annulus is a separate population of circular fibrils. (*E*) Linear belts of collagen (*solid lines*) run from limbus to limbus, leading to a two-dimensional projection view (*broken lines*) characterized by central orthogonal and peripheral annular fibrils. (*F*) Confocal elliptic/hyperbolic model in which fibrils loop around nasal and temporal foci. Redrawn from (*A–D*) Meek and Boote (21), (*E*) Pinsky et al. (23), and (*F*) Misson (24).

WAXS images were collected along the two principal cardinal and oblique corneal meridians at intervals of 0.5 mm (central 7 mm) or 0.05 mm (7 mm to scleral edge), as shown in Fig. 3 *A*. To verify the results, four principal corneal semimeridians were examined in Cornea 2 (Fig. 3 *B*). X-ray exposure time was 3 s (Cornea 1) or 0.5 s (Cornea 2). Exposure time for Cornea 2 was reduced to avoid tissue damage when using a more finely focused beam of the same energy. Precise vertical/horizontal specimen translation between exposures was achieved using a computer-controlled motor stage. The resulting WAXS images were recorded on a FReLoN CCD detector (ESRF-ISG, Grenoble, France) placed ~20 cm behind the specimen.

The corneal WAXS pattern (Fig. 3 *C*) contains a reflection deriving from the regular lateral spacing (~1.6 nm in humans) of collagen molecules lying near-axially within the stromal fibrils (6). The fibrils in a given lamella scatter x-rays in a direction perpendicular to their long axes, forming two symmetrical diffraction maxima on the detector. A line normal to that joining the two maxima thereby indicates the fibril direction, whereas the peak intensity is proportional to the number of fibrils aligned in that direction. Hence, from the angular distribution of WAXS intensity, any
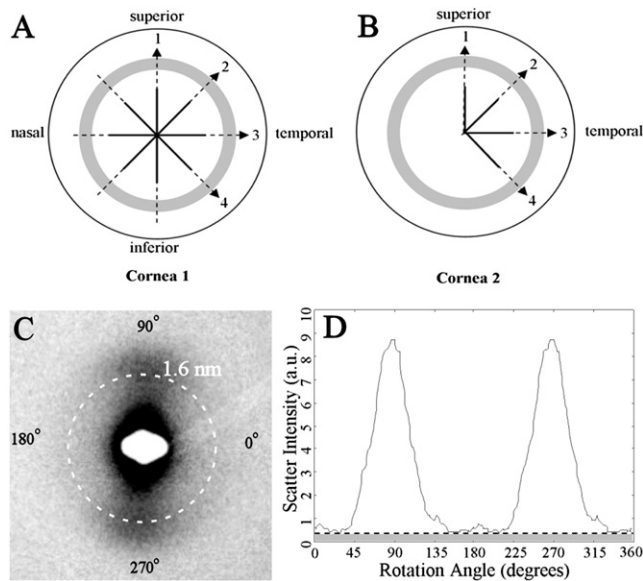
FIGURE 3 (*A* and *B*) Scan lines on the two left human corneoscleral buttons used for microfocus WAXS. Solid line: coarse sampling (0.5 mm); broken line: fine sampling (0.05 mm). Shaded region denotes the limbus. (*C*) WAXS pattern from the limbal region of Cornea 1, showing the collagen intermolecular WAXS reflection centered at 1.6 nm. (*D*) Normalized x-ray scatter from fibrillar collagen as a function of rotation angle. Each of the 256 values in the distribution is extracted via a radial integration of the (background-subtracted) collagen WAXS peak. The clear region corresponds to preferentially aligned collagen, whereas the shaded region corresponds to isotropic collagen.

preferential fibril orientation may be detected, and the relative number of fibrils oriented in any direction within the corneal plane quantified (5).

Intensity values were extracted using a combination of Optimas 6.5 (Media Cybernetics, Marlow, UK) and Excel (Microsoft, Reading, UK) software. Data were normalized against fluctuations in incident beam current using electronically recorded readings from an ion chamber placed before the specimen. Scatter from air, Clingfilm, and other corneal components other than fibrous collagen was removed by fitting and subtracting a two-dimensional power law background function. Fig. 3 *D* shows the resulting scatter intensity distribution, plotted as a function of angle around the WAXS reflection. Intensity values were extracted to 256 equally spaced bins, each representing an angular sector of 1.4°. The scatter component from preferentially aligned fibrils (Fig. 3 *D*; *clear region*) was isolated from that arising from the isotropically arranged collagen (Fig. 3 *D*; *shaded region*) and the peak positions and peak scatter intensities measured to determine the preferred angle and relative number of fibrils lying within a 1.4° sector of this angle, respectively. The relative contribution of isotropic collagen was also calculated for a 1.4° sector. This was repeated for all the sampling locations indicated in Fig. 3, *A* and *B*, enabling us to monitor the size and direction of the two principal fibril populations (centrally: i-s and n-t), and the contribution of isotropic collagen, as a function of radial distance from the corneal center. We thereby obtained quantitative information on the course of collagen fibrils over the corneolimbal junction at a spatial resolution of 50 μm. The relative proportion of the two aligned fibril populations and the isotropic collagen were calculated for the central cornea, inner limbal edge, and limbal center by dividing the individual peak scatter values of each population by the total of all three. Peak scatter was calculated for the central cornea as an average of values within the central 6 mm, whereas a 9-point moving average algorithm was employed to extract representative values from the higher spatially resolved peripheral data for the inner limbal edge and limbal center.

Small-angle x-ray scattering

Small-angle x-ray scattering (SAXS) data were collected from Corneas 3 and 4 on beamline I22 at the Diamond Light Source (Didcot, UK), using an x-ray beam ($\lambda = 0.10$ nm), measuring 0.2 mm in diameter. The use of a conventional (rather than microfocus) beam enabled greater sampling/averaging of the tissue at each datapoint, reducing signal noise for accurate measurement of SAXS fibril transform peaks and therefore quantification of fibril diameters, as described below. Corneal mounting followed that described for WAXS experiments above. SAXS images resulting from a beam exposure of 10 s were collected during radial scans along the four principal corneal meridians at intervals of 0.5 mm from limbus to limbus, as shown in Fig. 4 *A*. Specimen alignment was achieved by an initial exposure of x-ray sensitive film placed in the specimen holder to locate the incident beam position.

The equatorial (perpendicular to the fibril axis) corneal SAXS pattern contains information about the average separation and diameter of collagen fibrils within the volume of stroma traversed by the x-ray beam (6). The intensity distribution, I(**K**), of the pattern is given by the product of scattering from an individual fibril, termed the fibril transform F(**K**), and that arising from the relative fibril positions, termed the interference function G(**K**), plus an additional background of noncollagen scatter, B(**K**):

$$I(\mathbf{K}) = F(\mathbf{K})G(\mathbf{K}) + B(\mathbf{K}). \tag{1}$$

Here, **K** is the scattering vector, whose magnitude is defined in terms of the x-ray wavelength, λ, and scattering angle 2θ:

$$K = (4\pi/\lambda) \sin \theta. \tag{2}$$

From diffraction theory (25), and approximating collagen fibrils as infinitely long cylinders, the fibril transform is related to the fibril radius, r_f, by

$$F(Kr_f) = \left[2 J_1(Kr_f)/Kr_f\right]^2, \tag{3}$$

where J_1 is a Bessel function of the first order.

For each SAXS pattern (Fig. 4 *B*) a radial intensity profile (Fig. 4 *C*) was extracted using a combination of Fit2d (ESRF) and Excel software. A power-law background function, representing B(K), was then fitted (Fig. 4 *C*) and subtracted using in-house software based on Python 2.6 (Python Software Foundation, Wolfeboro Falls, NH). The same program was then used to fit a fibril transform function (Fig. 4 *D*), of the form of Eq. 3. The average collagen fibril diameter, $2r_f$, was then calculated from the first subsidiary maximum position of F(Kr_f) (Fig. 4 *D*; *solid arrow*), which occurs at $Kr_f = 5.14$ (6). In this region of the scattering pattern (and at higher K) the contribution of G(K) is negligible (26), and it was therefore ignored in the calculations. Calibration of K was achieved using the 67 nm meridional reflection from a SAXS pattern of hydrated rat tail tendon.

RESULTS

Preferential collagen fibril orientation across the corneolimbal interface

Fibril angle

Along the vertical and horizontal corneal meridians, the two principal aligned fibril populations remained largely orthogonal from central cornea to limbus (see Fig. 5, *A* and *E*, and Fig. 6, *A* and *E*), with net rotation between corneal center and limbal center, as an average of the 2 corneas, being 4° for n-t and −1° for i-s fibrils. Exceptionally, in the case of Cornea 1, a 22° rotation of i-s fibrils was observed as the superior inner limbal edge was approached (Fig. 5 *A*).
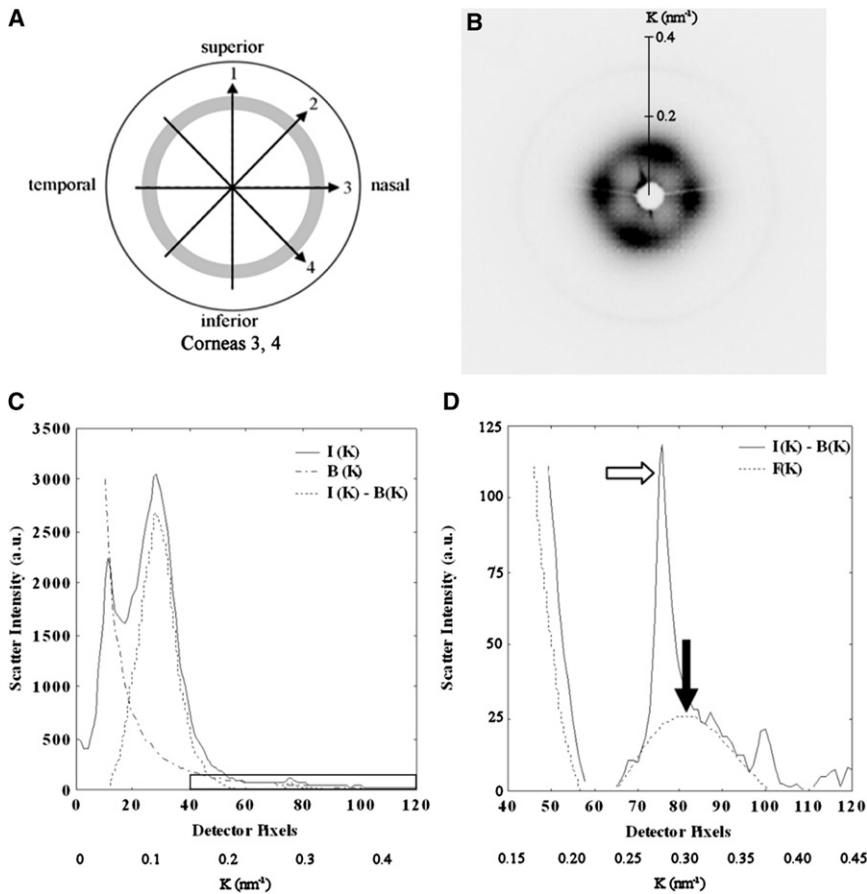
FIGURE 4 (*A*) Scan lines on the two right human corneoscleral buttons used for SAXS. The sampling interval was 0.5 mm and the shaded region denotes the limbus. (*B*) SAXS pattern from the center of Cornea 3. (*C*) Vertical intensity profile, I(K), through pattern shown in *B*. The data is folded about the pattern center. A background function, B(K), is subtracted. The collagen inter-ference function peak arising from the short-range lateral order of the stromal fibrils can be clearly seen. The region bounded by the rectangular box is shown expanded in *D*. (*D*) A fibril transform function, F(K), is fitted to the background-sub-tracted data and the peak position (*solid arrow*) calibrated to determine the average collagen fibril diameter. The sharp third order collagen meridi-onal peak (*empty arrow*) is visible merged into the equatorial pattern, and may be ignored in fitting the fibril transform.

However, this rotation was reversed in the limbus itself, with an orthogonal arrangement being restored at the limbal center. In addition a $-12°$ change in the direction of n-t fibrils was noted in moving from corneal center to the temporal limbal center (see Fig. 5 *E*). These two latter observations are likely to be attributable to minor artifact caused by inaccuracy in centering and/or aligning the rota-tion of Cornea 1 before scanning, because they were not observed in the fibril angle results from either Cornea 2 (see Fig. 6, *A* and *E*) or a third left human cornea subse-quently examined (data not shown). In contrast to the vertical and horizontal scans, when approaching the limbus along the diagonal corneal meridians (see Fig. 5, *C* and *G*, and Fig. 6, *C* and *G*), in most cases a gradual rotation of both fibril populations was measured over the peripheral-most 1–1.5 mm of the cornea. This rotation continued into the limbus in some scans and, in every case, the two fibril populations had coaligned tangential to the cornea on reach-ing the limbal center. Net rotation for diagonal scans, as an average of the two corneas, was $-46°$ for n-t and $35°$ for i-s fibrils. The abrupt coming together of data points for the final ~0.5mm of the transition is because once peak separa-tion became $< 30°$, the peaks were nonresolvable and considered as a single, merged peak. This point was desig-

nated as coalignment of the two populations, and it was assumed that the two aligned fibril populations made an equal contribution to the merged peak in subsequent peak intensity measurements.

Fibril number

Along the vertical corneal meridian (see Fig. 5 *B* and Fig. 6 *B*), scatter due to i-s fibrils remained essentially constant across the central 5 mm of the cornea. In the final 2 mm of the cornea up until the limbus, intensity either stayed the same (Cornea 2) or increased slightly (Cornea 1). Over the central 5 mm, n-t fibril peak scatter remained comparable with the i-s population. However, in the final 2 mm of the cornea before the limbus the n-t population began to domi-nate and, at the limbal center, these fibrils out-numbered the i-s population by a factor of 1.5 for Cornea 1 (Fig. 5 *B* and Table 1). In Cornea 2 the preponderance of the n-t fibrils in the corneal periphery was even greater, such that the i-s fibril peak could not be detected past the inner limbal edge (Fig. 6 *B*), at which point the relative proportions were 2.2:1 in favor of the n-t population (Table 1). Notably, when traversing the corneolimbal interface along the hori-zontal direction (see Fig. 5 *F* and Fig. 6 *F*) the reverse effect was observed, in which the i-s fibrils began to dominate over
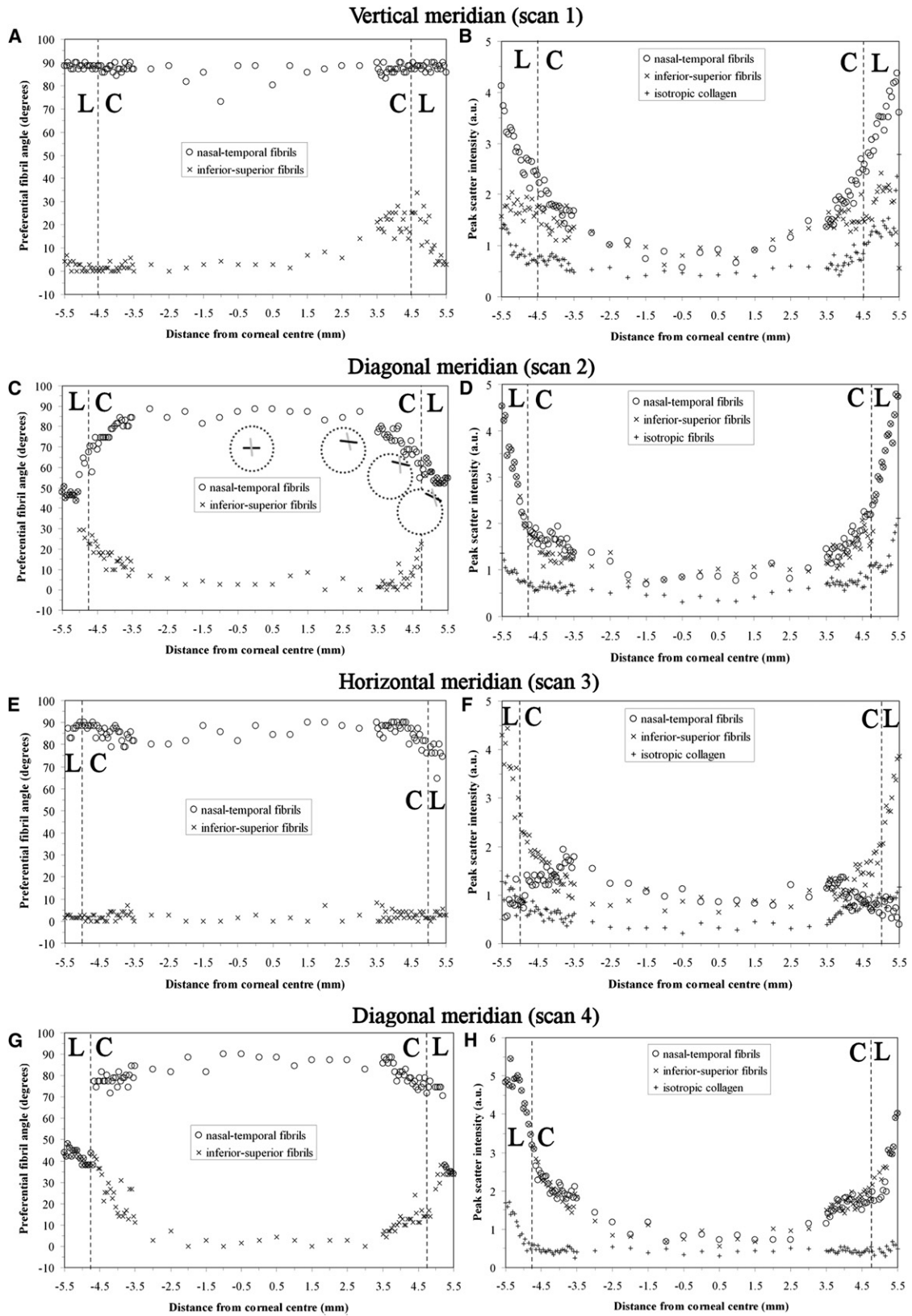
FIGURE 5 (A, C, E, and G) Preferential angle of (*centrally*) i-s and n-t aligned fibril populations, as a function of distance from corneal center for Cornea 1. (B, D, F, and H) Peak x-ray scatter for aligned and isotropic fibril populations. The corneal, C, and limbal, L, regions are indicated. Insets in C depict line plots representing the local direction of n-t (*black line*) and i-s (*gray line*) populations at four selected points along diagonal scan 2.
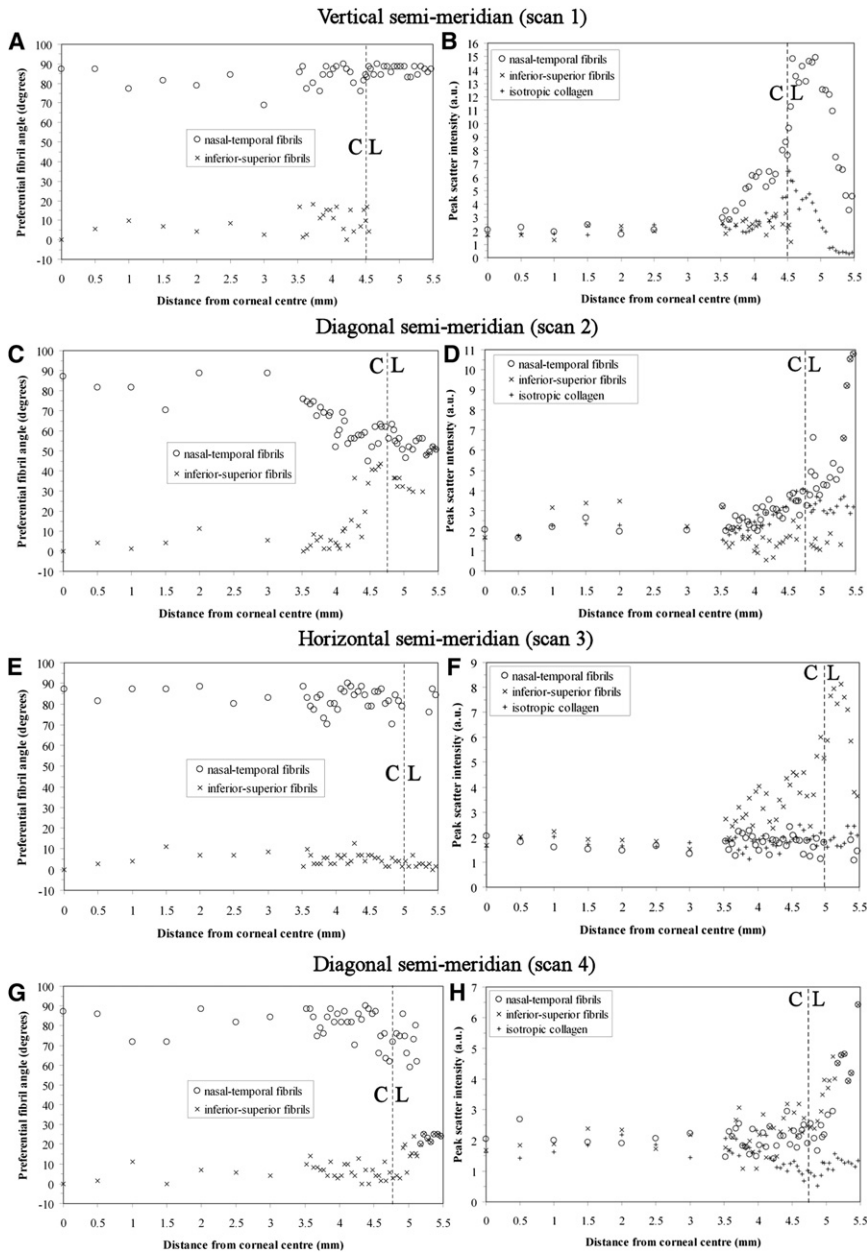
FIGURE 6 (*A*, *C*, *E*, and *G*) Preferential angle of aligned fibril populations for Cornea 2. (*B*, *D*, *F*, and *H*) Peak x-ray scatter for aligned and isotropic fibril populations. The corneal, C, and limbal, L, regions are indicated.

the n-t population, again beginning 1–1.5mm from the limbus, with their relative proportions being 6.3:1 for Cornea 1 and 4.1:1 for Cornea 2 at the limbal center (Table 1). Although i-s fibrils dominated in the proximity of the limbus for horizontal scans, a small increase in n-t fibrils was observed in Cornea 1 (Fig. 5 *F*).

For diagonal scans, both i-s and n-t fibril populations showed an increase in occupancy over the final 1 mm before the limbus for Cornea 1 (see Fig. 5, *D* and *H*). In Cornea 2, a similar increase in occupancy was measured over the same region for either n-t (Fig. 6 *D*) or i-s (Fig. 6 *H*) fibrils, depending on scan direction. In all diagonal scans this increase continued at a similar rate up until the limbus, where it

began to rise more sharply across the limbus itself, likely as a result of the gradual merging of the peaks as the two populations coaligned along a direction tangential to the limbus (Fig. 5, *D* and *H*, and Fig. 6, *D* and *H*).

In contrast to the case for aligned collagen, isotropic scatter generally remained constant across the cornea, increasing significantly only within the limbus itself (Fig. 5, *B*, *D*, *F*, and *H*, and Fig. 6, *B*, *D*, *F*, and *H*). The exceptions to this were for scan 3 of Cornea 1 (Fig. 5 *F*) and scan 2 of Cornea 2 (Fig. 6 *D*). Notably, Cornea 2 featured a consistently higher proportion of isotropic collagen compared to Cornea 1 in all examined locations, this parameter measuring, on average, 63%, 61%, and

TABLE 1 Relative proportion of fibrils occupying a 1.4° sector around the preferential alignment direction for aligned and isotropic, iso, fibril populations at three locations

Scan - location on limbus (Cornea #)	Relative proportions of fibril populations by location								
	Cornea (central 6mm)			Inner limbal edge			Limbal center		
	i-s	n-t	iso	i-s	n-t	iso	i-s	n-t	iso
1 - inf (1)	–	–	–	0.36	0.48	0.16	0.34	0.50	0.16
- sup (1)	0.41	0.40	0.19	0.31	0.52	0.17	0.31	0.50	0.19
- sup (2)	0.36	0.33	0.31	0.21	0.47	0.32	†	0.78	0.22
2 - inf-nas (1)	–	–	–	0.40	0.45	0.15	0.39*	0.39*	0.22
- sup-temp (1)	0.41	0.39	0.20	0.35	0.45	0.20	0.37*	0.37*	0.26
- sup-temp (2)	0.38	0.31	0.31	0.21	0.38	0.41	0.34*	0.34*	0.32
3 - nas (1)	–	–	–	0.58	0.21	0.21	0.68	0.11	0.21
- temp (1)	0.39	0.45	0.16	0.52	0.23	0.25	0.70	0.11	0.19
- temp (2)	0.36	0.33	0.33	0.60	0.18	0.22	0.65	0.16	0.19
4 - sup-nas (1)	–	–	–	0.43*	0.43*	0.14	0.37*	0.37*	0.25
- inf-temp (1)	0.39	0.41	0.20	0.47	0.41	0.12	0.45*	0.45*	0.10
- inf-temp (2)	0.35	0.36	0.29	0.43	0.38	0.19	0.39	0.39	0.22

* Indicates coalignment of i-s and n-t populations, where each population was assumed to contribute equally to the combined peak. † indicates peak was not measurable due to low fibril occupancy.

20% higher in the central cornea, inner limbal edge and limbal center, respectively (Table 1). It is possible that this observation may be age-related, since the donor ages were 27 years apart. Although there is no documented evidence to suggest that the preferential orientation of corneal lamellae alters with age, it is conceivable that age-related changes in stromal collagen packing at the intra- and inter-fibrillar level (27) might impact on the overall intensity of WAXS scatter observed between Corneas 1 and 2.

The distribution of collagen fibril diameters from central cornea to limbus

Collagen fibril diameter from SAXS measurements is plotted as a function of distance from the corneal center in Fig. 7. Fibril diameter was observed to remain constant within the central 6 mm of both Cornea 3 (Fig. 7 A) and Cornea 4 (Fig. 7 B). The average diameter for the central 6 mm is given in Table 2. The larger central fibril diameter for Cornea 3 is likely due to this specimen being from a donor 23 years older than Cornea 4, as previous studies have shown that the diameter of corneal collagen fibrils increases with age (27).
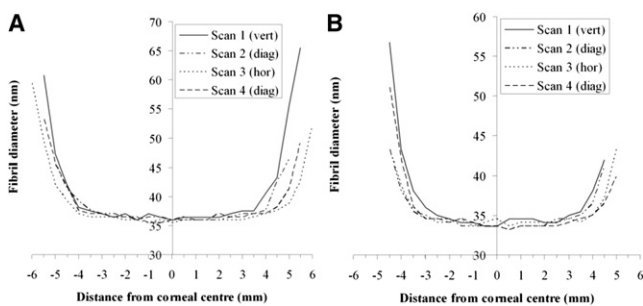

FIGURE 7 Average collagen fibril diameter as a function of distance from the corneal center for (A) Cornea 3 and (B) Cornea 4.

Fibril diameter was observed to increase sharply outside the central 6 mm in all scans (Fig. 7). To further test our hypothesis that the peripheral human cornea and limbus is reinforced by (larger) collagen fibrils of scleral origin in the manner shown in Fig. 1 B, we determined the distance from the corneal center at which the increase in fibril diameter became significant. This point of significant increase was defined as the average distance (of the 2 points either side of the center) at which the difference between individual fibril diameter measurements and the average value for the central 6 mm became >2 standard deviations of the latter. These values are shown in Table 2, alongside the equivalent values predicted by the theoretical model of Fig. 1 B.

DISCUSSION

A number of conventional x-ray scattering studies have yielded information on the course of corneal and limbal collagen (5). The finest spatial resolution obtained by these methods was 0.2 mm (22). With the recent advent of micro-beam x-ray technology, it has become possible to gain a more detailed picture of tissue structure at resolutions in the micron range, and in a preliminary study we obtained x-ray data at 0.025 mm spatial intervals from the corneolimbal interface along 1 vertical and 1 oblique semimeridian of a human eye (21). The current work expands considerably on this by examining the corneolimbal interface along all eight of the principal cardinal and oblique semimeridians, quantifying the angle and relative proportions of the two major aligned fibril populations, along with the contribution of isotropic collagen. It should be noted that in this highly simplified view of the cornea we do not consider the degree of dispersion of fibrils around the preferred alignment directions, which previous WAXS studies have shown to vary with position in the peripheral cornea and limbus (5). Moreover, we have not here quantified additional fibril

TABLE 2   Average fibril diameter (and standard deviation) across the central 6 mm, alongside the position of significant increase, the average distance from the corneal center at which the observed increase in fibril diameter with proximity to the limbus became significant

	Avg. Fibril diameter (central 6 mm), nm		Position of significant increase, mm			
Scan (direction)	Cornea 3	Cornea 4	Cornea 3	Cornea 4	Avg.	Model
1 (vert)	36.7(± 0.5)	34.4(± 0.6)	4.0	3.5	3.75(± 0.5)	3.5
2 (diag)	36.4(± 0.4)	33.9(± 0.5)	3.75	3.5	3.63(±0.3)	3.25
3 (hor)	36.0(± 0.3)	34.2(± 0.4)	4.0	4.0	4.0(±0.4)	4.5
4 (diag)	36.3(± 0.5)	33.9(± 0.4)	4.25	3.75	4.0(±0.4)	4.0

Also shown is the position of significant increase value predicted by the model of Fig. 1 *B*, in which larger scleral fibrils are assumed to reinforce the peripheral oblique cornea. Note that the model predicts lower POSI values for scans 1 and 2 compared to 3 and 4, consistent with the current data.

subpopulations in the peripheral cornea, the presence of which are implied by the frequent presence of subpeaks in the WAXS intensity distribution graphs recorded over the corneolimbal transition zone. This effect may stem from the extensive branching of lamellae in the peripheral cornea, as indicated by scanning electron microscopy (28). However, despite these limitations, the current study has enabled us to gain new (to our knowledge) detailed, quantitative information on the structure of the corneolimbal junction. The data indicate that, for a given specimen, the manner of integration of the corneal and limbal fibrils is not circularly symmetrical, but rather varies significantly depending on the direction along which the limbus is approached. This may be an important factor governing the corneal response to surgeries that involve peripheral incisions, for example cataract operation. Specifically, in light of the current data, it is interesting to note that astigmatic changes resulting from perilimbal corneal incision vary in magnitude depending on the circumferential location at which the cut is made (29).

Although the corneolimbal junction is evidently a highly complex structure, a number of general features may be identified from the current data. The reinforcement of the vertical fibrils on approaching the nasal/temporal limbus, along with an increase in horizontal fibrils with proximity to the superior/inferior limbus, was a notable result of this study. Taken together with the presence of tangential collagen observed in all oblique limbal regions, these results are consistent with the presence of a pseudoannulus of collagen circumscribing the cornea, in agreement with previous x-ray (9) and anatomical (11,30) evidence. The question arises as to whether the limbal annulus is a discrete population of fibrils, as shown in Fig. 2, *B–D*, or alternatively arises solely from a realignment of the central orthogonal fibrils (Fig. 2 *A*), or is a combination of the two. Although there is evidence of discrete annular structures residing in the posterior stroma of the limbal region (10,11), the gradual nature of the change in the preferred angle of the i-s and n-t aligned fibrils along the diagonal corneal meridians, such that they combine in a tangential orientation, strongly indicates that at least a portion of the central orthogonal fibrils must change direction somehow

to fuse with the limbal fibrils, since the angular change would be expected to be considerably more abrupt if the limbal annulus were a totally separate structure. Such a continuous bulk change in fibril direction, which might be achieved via the repeated splitting and fusing of lamellae (28), would not, however, support the confocal elliptic/hyperbolic scheme (Fig. 2 *F*) envisaged by Misson (24).

Pinsky et al. (23) propounded an alternative model of the cornea to explain the results of conventional x-ray scattering experiments, in which orthogonal linear belts of collagen run uninterrupted from limbus to limbus, forming a geodesic dome structure (Fig. 2 *E*). Although this model is entirely consistent with a two-dimensional projected view of the cornea (such as that provided by x-ray scattering) featuring central orthogonal and peripheral circular fibrils, it appears at odds with the concept of the two structures integrating via the fusing/splitting of lamellae, as suggested by scanning electron microscopy (28). Moreover, the geodesic model cannot account for the reinforcement of the peripheral collagen indicated by the current study. While, from the current data, the central orthogonal and peripheral tangential fibrils appear to fuse, the latter are clearly reinforced by additional collagen proximal to, and continuing into, the limbus. Peak x-ray scatter from aligned collagen was observed to increase some 2.5–3.5 mm from the corneal center, depending on direction, whereas the increase in scatter from nonaligned collagen was mainly restricted to the limbus. This suggests that the increase in peripheral corneal thickness, which also commences some 2.5–3.5 mm from the corneal center, and is also direction dependent in nature (31), is in major part due to the presence of additional aligned (as opposed to isotropic) collagen. In contrast, the present results indicate that the further increase in stromal thickness at the limbus (31,32) is likely due to a significant number of additional lamellae equally disposed in all directions within the corneal plane, along with a portion adopting a (mainly tangential) preferred orientation.

From where might the additional aligned collagen that reinforces the peripheral cornea and limbus originate? At the limbus itself, a large proportion of the additional scatter is likely to be attributable to additional tangential/circular lamellae residing in the posterior stroma (10,11). However,

this does not explain the increase we observe as close as 2.5 mm from the corneal center. An interesting result of the current study was that, in addition to the increase in tangential collagen consistent with the presence of the limbal annulus, in approaching the cardinal points of the limbus, radial fibril scatter was also observed to increase (e.g., vertical fibrils near the inferior/superior limbus of Cornea 1). We also noted this effect in our preliminary microfocus study (21). Given there is ample evidence from fibril diameter (14,15) and transparency (16) measurements that peripheral corneal collagen in the human eye intermingles with the larger scleral fibrils, we propose that fibrils originating in the sclera must enter and leave the peripheral cornea without entering the central 6 mm. Moreover, because additional radially aligned collagen appears to enter at the cardinal points of the limbus, but does not continue into the central 6 mm, this collagen must either terminate mid cornea, or else follow a curved path, exiting the cornea at another circumferential point. Microscopy has revealed that a proportion of the anterior-most corneal lamellae terminate by suturing into Bowman's layer (33,34). However, notably, previous x-ray scattering work has indicated that the preferential orientation of lamellae within the corneal plane is, in major part, restricted to the posterior one-third of the stromal thickness (10,35), and it may therefore be within the deeper layers of the peripheral cornea that the reinforcing collagen of possible scleral origin resides.

Previously, we obtained from conventional WAXS experiments (12,13) complete contour maps of aligned collagen scatter for human corneas, which indicated enhanced reinforcement of the oblique corneal periphery (Fig. 1 A), and we speculated may relate to anchoring collagen of scleral origin (Fig. 1 B). This scatter contour pattern was found to be highly conserved in the human eye, and to show a high degree of midline symmetry between fellow eyes (13), to the extent that a cornea may be identified as left or right by the shape of this pattern alone. If these anchoring scleral fibrils exist, then we might expect this to be reflected in the distribution of bulk-thickness fibril diameter from central cornea to limbus. Specifically, with reference to Fig. 1 B, we may expect the fibril diameter to begin to increase at a point closer to the corneal center along the inferior/superior and inferotemporal/superonasal meridians compared with the other directions. However, diameter measurements so far have been restricted to either a single vertical scan (15) or two orthogonal, cardinal scans through the cornea (14). In the current study, we have obtained the missing oblique information (Fig. 7), and reference to Table 2 shows that the present data are indeed consistent with the model of the right cornea shown in Fig. 1 B, i.e., point of significant increase values for scans 1 and 2 were on average lower than the equivalent values for scans 3 and 4. A schematic model of the possible integration of the corneal, limbal, and scleral fibrils in the right human eye, based on the results of the current study, is shown in Fig. 8.
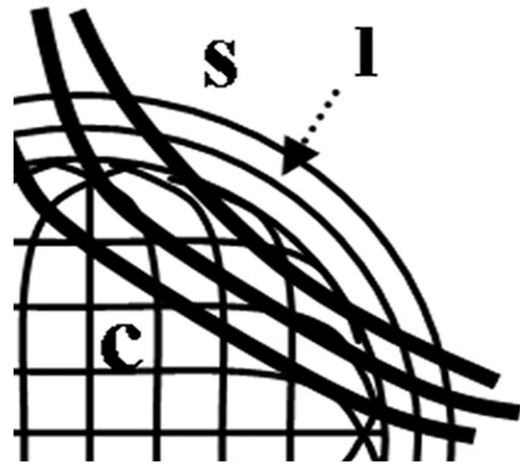

FIGURE 8 Schematic showing possible integration of the corneal, c, and limbal, l, collagen fibrils in the right human eye, based on the current x-ray data (superonasal quadrant shown). Centrally orthogonal fibrils change direction in the peripheral cornea to fuse with the tangential fibrils of the highly reinforced limbal annulus. Chords of larger anchoring fibrils, originating in the sclera, s, cross the oblique peripheral cornea.

CONCLUSION

The results of this study show that the manner of integration and reinforcement of the corneal and limbal collagen fibrils of the human eye is not circularly symmetrical, but instead varies markedly depending on the direction along which the limbus is approached. Of importance, this implies that the corneal biomechanical response to peripheral surgical incisions may be different, depending on the location at which the incision is made. This may relate to clinical observations reporting differences in the magnitude of corneal astigmatism associated with different incision points (29). Although x-ray scattering is a powerful technique for obtaining quantitative structural information on corneoscleral collagen, it should be remembered that all the conclusions drawn in this work relate to bulk thickness data. Although depth-profiled x-ray data can be obtained via serial tissue sections (10,35), resolution in the stromal depth plane is inevitably limited. The wide-field imaging techniques, in particular second harmonic generation multiphoton microscopy (10,33), continue to provide a visual and, moreover, depth-resolved view of the corneal stroma, complimentary to the quantitative x-ray measurements presented here. Together these techniques have the potential to build a detailed picture of the human corneal stroma in three dimensions.

REFERENCES

1. Maurice, D. M. 1957. The structure and transparency of the cornea. *J. Physiol.* 136:263–286.

2. Komai, Y., and T. Ushiki. 1991. The three-dimensional organization of collagen fibrils in the human cornea and sclera. *Invest. Ophthalmol. Vis. Sci.* 32:2244–2258.

3. Fatt, I., and B. Weissman. 1992. Physiology of the Eye: An Introduction to the Vegetative Functions. Butterworth-Heinmann, Boston, MA.

4. Meek, K. M. 2009. Corneal collagen—its role in maintaining corneal shape and transparency. *Biophys. Rev.* 1:83–93.

5. Meek, K. M., and C. Boote. 2009. The use of x-ray scattering techniques to quantify the orientation and distribution of collagen in the corneal stroma. *Prog. Retin. Eye Res.* 28:369–392.

6. Meek, K. M., and A. J. Quantock. 2001. The use of x-ray scattering techniques to determine corneal ultrastructure. *Prog. Retin. Eye Res.* 20:95–137.

7. Boote, C., S. Dennis, …, K. M. Meek. 2005. Lamellar orientation in human cornea in relation to mechanical properties. *J. Struct. Biol.* 149:1–6.

8. Daxer, A., and P. Fratzl. 1997. Collagen fibril orientation in the human corneal stroma and its implication in keratoconus. *Invest. Ophthalmol. Vis. Sci.* 38:121–129.

9. Newton, R. H., and K. M. Meek. 1998. Circumcorneal annulus of collagen fibrils in the human limbus. *Invest. Ophthalmol. Vis. Sci.* 39:1125–1134.

10. Kamma-Lorger, C. S., C. Boote, …, K. M. Meek. 2010. Collagen and mature elastic fibre organisation as a function of depth in the human cornea and limbus. *J. Struct. Biol.* 169:424–430.

11. Hogan, M. J., and J. Alvarado. 1969. Ultrastructure of the deep corneo-limbal region. *Doc. Ophthalmol.* 26:9–30.

12. Aghamohammadzadeh, H., R. H. Newton, and K. M. Meek. 2004. X-ray scattering used to map the preferred collagen orientation in the human cornea and limbus. *Structure.* 12:249–256.

13. Boote, C., S. Hayes, …, K. M. Meek. 2006. Mapping collagen organization in the human cornea: left and right eyes are structurally distinct. *Invest. Ophthalmol. Vis. Sci.* 47:901–908.

14. Boote, C., S. Dennis, …, K. M. Meek. 2003. Collagen fibrils appear more closely packed in the prepupillary cornea: optical and biomechanical implications. *Invest. Ophthalmol. Vis. Sci.* 44:2941–2948.

15. Borcherding, M. S., L. J. Blacik, …, H. G. Weinstein. 1975. Proteoglycans and collagen fibre organization in human corneoscleral tissue. *Exp. Eye Res.* 21:59–70.

16. Doutch, J., A. J. Quantock, …, K. M. Meek. 2008. Light transmission in the human cornea as a function of position across the ocular surface: theoretical and experimental aspects. *Biophys. J.* 95:5092–5099.

17. Asejczyk-Widlicka, M., D. W. Sródka, …, B. K. Pierscionek. 2007. Modelling the elastic properties of the anterior eye and their contribution to maintenance of image quality: the role of the limbus. *Eye (Lond.).* 21:1087–1094.

18. Boote, C., S. Hayes, …, K. M. Meek. 2009. Ultrastructural changes in the retinopathy, globe enlarged (rge) chick cornea. *J. Struct. Biol.* 166:195–204.

19. Maurice, D. M. 1984. The cornea and sclera. *In* The Eye. H. Davson, editor. Academic Press, Orlando, FL. 1–158.

20. Quantock, A. J., S. Dennis, …, M. Tachibana. 2003. Annulus of collagen fibrils in mouse cornea and structural matrix alterations in a murine-specific keratopathy. *Invest. Ophthalmol. Vis. Sci.* 44:1906–1911.

21. Meek, K. M., and C. Boote. 2004. The organization of collagen in the corneal stroma. *Exp. Eye Res.* 78:503–512.

22. Newton, R. H., and K. M. Meek. 1998. The integration of the corneal and limbal fibrils in the human eye. *Biophys. J.* 75:2508–2512.

23. Pinsky, P. M., D. van der Heide, and D. Chernyak. 2005. Computational modeling of mechanical anisotropy in the cornea and sclera. *J. Cataract Refract. Surg.* 31:136–145.

24. Misson, G. P. 2007. Circular polarization biomicroscopy: a method for determining human corneal stromal lamellar organization in vivo. *Ophthalmic Physiol. Opt.* 27:256–264.

25. Oster, G., and G. P. Riley. 1952. Scattering from cylindrically symmetric systems. *Acta Crystallogr.* 5:272–276.

26. Worthington, C. R., and H. Inouye. 1985. X-ray diffraction study of the cornea. *Int. J. Biol. Macromol.* 7:2–8.

27. Daxer, A., K. Misof, …, P. Fratzl. 1998. Collagen fibrils in the human corneal stroma: structure and aging. *Invest. Ophthalmol. Vis. Sci.* 39:644–648.

28. Radner, W., M. Zehetmayer, …, R. Mallinger. 1998. Interlacing and cross-angle distribution of collagen lamellae in the human cornea. *Cornea.* 17:537–543.

29. Altan-Yaycioglu, R., A. Pelit, …, Y. A. Akova. 2007. Astigmatism induced by oblique clear corneal incision: right vs. left eyes. *Can. J. Ophthalmol.* 42:557–561.

30. Kokott, W. 1938. The mechano-functional structure of the eyes. *Albrecht Von Graefes Arch. Ophthalmol.* 138:424–485.

31. Reinstein, D. Z., M. Gobbe, …, B. Bloom. 2009. Epithelial, stromal, and corneal pachymetry changes during orthokeratology. *Optom. Vis. Sci.* 86:E1006–E1014.

32. Hamada, R., J. P. Giraud, B. Graf, and Y. Pouliquen. 1972. Analytical and statistical study of the lamellae, keratocytes and collagen fibrils of the central region of the normal human cornea. (Light and electron microscopy). *Arch. Ophtalmol. Rev. Gen. Ophtalmol.* 32:563–570.

33. Jester, J. V., M. Winkler, …, D. J. Brown. 2010. Evaluating corneal collagen organization using high-resolution nonlinear optical macroscopy. *Eye Contact Lens.* 36:260–264.

34. Morishige, N., W. M. Petroll, …, J. V. Jester. 2006. Noninvasive corneal stromal collagen imaging using two-photon-generated second-harmonic signals. *J. Cataract Refract. Surg.* 32:1784–1791.

35. Abahussin, M., S. Hayes, …, K. M. Meek. 2009. 3D collagen orientation study of the human cornea using x-ray diffraction and femtosecond laser technology. *Invest. Ophthalmol. Vis. Sci.* 50:5159–5164.